Available online at www.sciencedirect.com
SCIENCE DIRECT®
Journal of Solid State Chemistry 171 (2003) 334–338
JOURNAL OF SOLID STATE CHEMISTRY
http://elsevier.com/locate/jssc

Magnetic properties of $R-T$ hydrides (Ho, Y)$_6$Fe$_{23}$H$_{15}$

J. Ostoréro* and V. Paul-Boncour

Laboratoire de Chimie Metallurgique des Terres Rares, CNRS, UPR 209, 2 Rue Henri Dunant, 94320 Thiais Cedex, France

Received 24 April 2002; received in revised form 25 August 2002; accepted 28 August 2002

Abstract

Magnetization measurements $M(T,H,x)$ were performed on ferrimagnetic $Ho_{6-x}Y_xFe_{23}H_{15}$ ($x=0.47$ and 0.92) compounds in the 4.2–700 K temperature range (Curie temperature $T_C \sim 600$ K) in a magnetic field up to 55 kOe. In comparison to parent alloys, absorption of hydrogen leads to a decreasing compensation temperature, a strong increase of the magnetic moments of the compounds in the 200–400 K temperature range, and a higher Curie temperature. These results are analyzed within the frame of Herbst and Croat refined-Néel molecular field theory model, taking into account the increase of the iron magnetic moment and the weakening of the magnetic exchange coupling N_{Ho-Fe} as compared to their alloys values. The mean canting angle between rare earth and iron sublattices θ ($\theta \leqslant 10°$) is important for the yttrium-substituted compounds, particularly in the vicinity of compositions for which $T_{comp} \sim 0$ K.

Keywords: $R-T$ hydrides; Magnetic properties; Molecular field theory

1. Introduction

Among rare-earth (R)-transition metal (T) intermetallic compounds, iron-based alloys R_6Fe_{23} ($R=$ Gd−Yb) with a magnetic compensation temperature T_{comp} present a great interest for applications, e.g., thin films for high density magnetic and magnetooptic information recording media [1]. In bulk materials, absorption of hydrogen leads easily to the formation of hydrides of formula $R_6Fe_{23}H_z$ ($z<18$ under ordinary conditions) [2]. Most hydrides of the intermetallic compounds R_6Fe_{23} ($R=$ Ho, Y) retain the cubic $Fm3m$ host structure, R being located in site (24e), Fe occupying the four distinct positions (4b, 24d, 32f_1 and 32f_2), and H occupying the available interstitial sites [2–4]. Magnetic properties of pure R_6Fe_{23} hydrides were well studied in contrast to hydrides of substituted compounds. We presented recently the magnetic properties of yttrium-substituted Ho_6Fe_{23} intermetallic alloys [5]. In this paper, we present results of magnetic properties of cubic hydrides of formula $Ho_{6-x}Y_xFe_{23}H_z$ ($x=0.47$ and 0.92; $z=15$) obtained from these alloys. The "non-magnetic" yttrium substitutes Ho on the unique rare-earth site for both compounds. Concerning the magnetic properties of the end member $Ho_6Fe_{23}H_z$ ($x=0$; $z\leqslant 16$), magnetization measurements [6–7] and neutron diffraction experiments [8] show that the Fe moments are coupled ferromagnetically to each other and antiferromagnetically to the rare earth. At low temperature, the magnetic moment of Ho is close to its free ion value ($10\,\mu_B$ at.$^{-1}$) [8]. The experimental magnetic results of these pure ($x=0$) [6] and yttrium-substituted ferrimagnetic hydrides $Ho_{6-x}Y_xFe_{23}H_{15}$ ($x=0.47$ and 0.92) are analyzed within the frame of Herbst and Croat refined-Néel molecular field model [9].

2. Experimental

Intermetallic ingots of $Ho_{6-x}Y_xFe_{23}$ alloys were prepared by r.f. induction melting of the constituent metals in a water-cooled copper crucible, under a purified Ar atmosphere. The samples were remelted five times and vacuum annealed at 1100°C for 7 days in order to achieve homogeneity. The chemical composition was checked by X-ray diffraction and electron microprobe analysis. The samples studied were obtained for $x=0.47$ and 0.92. The hydrides $Ho_{6-x}Y_xFe_{23}H_z$ ($z=15\pm0.5$) were synthesized by reacting with

*Corresponding author. Fax: +33-1-4978-1203.
E-mail addresses: ostorero@glvt-cnrs.fr (J. Ostoréro), valerie.paul-boncour@glvt-cnrs.fr (V. Paul-Boncour).

0022-4596/03/$ - see front matter © 2003 Elsevier Science (USA). All rights reserved.
doi:10.1016/S0022-4596(02)00229-3

hydrogen gas at pressures below 1 MPa at 298 K using a Sievert apparatus [10]. X-ray diffraction powder experiments show that the compounds are single phase with cubic structure lattice parameters of 1.2400 nm ($x = 0.47$) and 1.2405 nm ($x = 0.92$). The corresponding cell volumes are greater than the limit of 1.8883 nm^3 below which the $R_6Fe_{23}H_z$ present a tetragonal distorsion [3]. Magnetization $M(H, T, x)$ measurements were performed on the powder samples from 4.2 to 700 K in a magnetic field up to 17 kOe using a Manics DSM8 magnetometer under pure helium atmosphere. Magnetic measurements, in a magnetic field up to 55 kOe, were also performed from 5 to 300 K on the $x = 0.47$ hydride sample using a SQUID magnetometer.

3. Results and discussion

3.1. Magnetization results below 300 K

We plotted in Figs. 1 and 2 the low temperature magnetization isotherms of the hydrides $Ho_{6-x}Y_xFe_{23}H_{15}$ corresponding to $x = 0.47$ and 0.92, respectively. For both samples and in the whole temperature range, "saturation" occurs for applied magnetic field $H > 6$ kOe. When temperature increases, for $x = 0.47$ (Fig. 1), the magnetization isotherms present a minimum at $T = 50$ K indicating the presence of a compensation temperature T_{comp}. The magnetization at T_{comp} is not proportional to the magnetic field as it should be for pure ferrimagnetic samples, indicating canted magnetic structures.

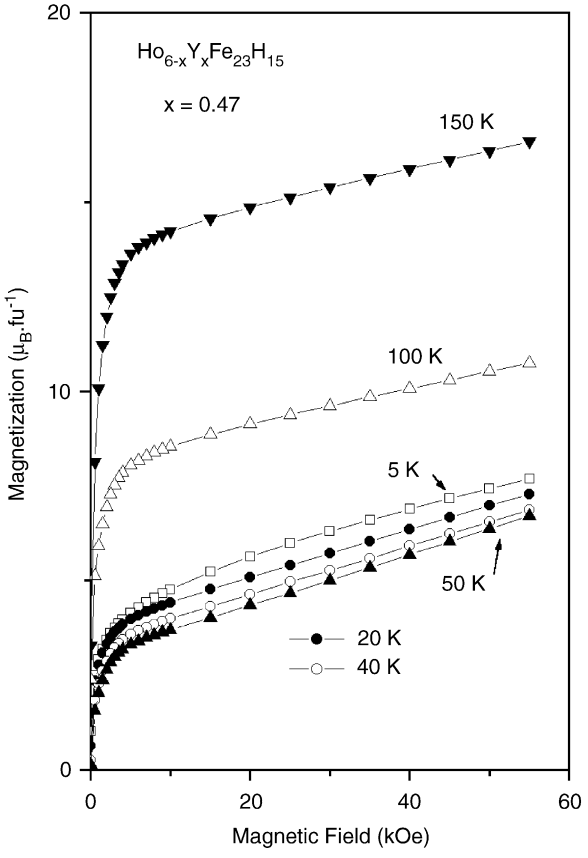

Fig. 1. Magnetization versus applied field of $Ho_{6-x}Y_xFe_{23}H_{15}$ ($x = 0.47$) compounds below room temperature.

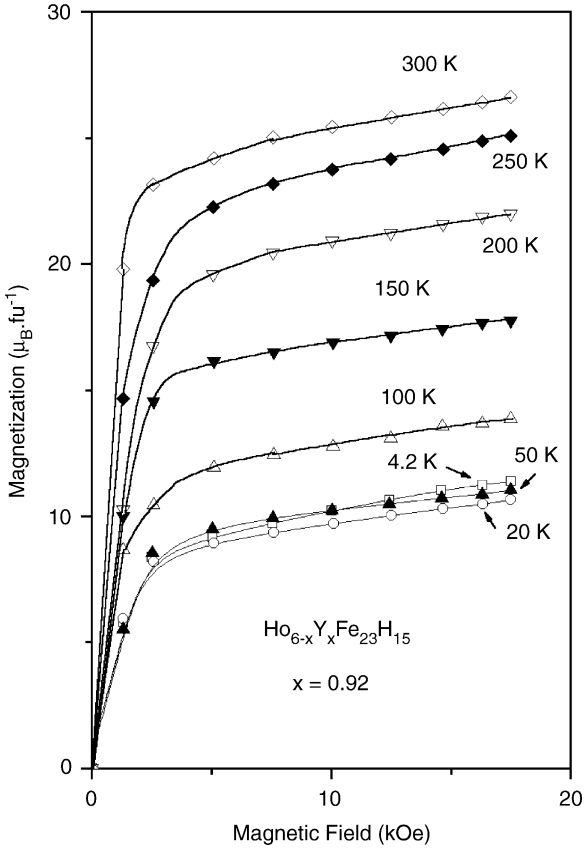

Fig. 2. Magnetization versus applied field of $Ho_{6-x}Y_xFe_{23}H_{15}$ ($x = 0.92$) compounds below room temperature.

For $x = 0.92$, in the 4.2–50 K temperature range, the difference between all magnetization isotherms is 7% or less (Fig. 2) which is at the limit of experimental accuracy ($\pm 3\%$). This precludes to conclude unambigously, at this stage, to the presence or absence of compensation temperature for $x = 0.92$ hydride compound.

The influence of hydrogenation on the magnetic properties is more evidenced in Fig. 3 ($x = 0.47$) and Fig. 4 ($x = 0.92$) where we plotted the isofield magnetization curves ($H = 16$ kOe) versus temperature for both hydrides and parent alloys. When $x = 0.47$, hydrogenation of the alloy leads to a compensation temperature shift of ~ -100 K (-6.7 K (at. H)$^{-1}$) (Fig. 3), close to the value ~ -110 K (-7.1 K (at. H)$^{-1}$) observed when $x = 0$ [6]. When $x = 0.92$, $T_{comp} = 99$ K [5] for the parent alloy. Assuming a shift of the order of -100 K after hydrogenation implies that the

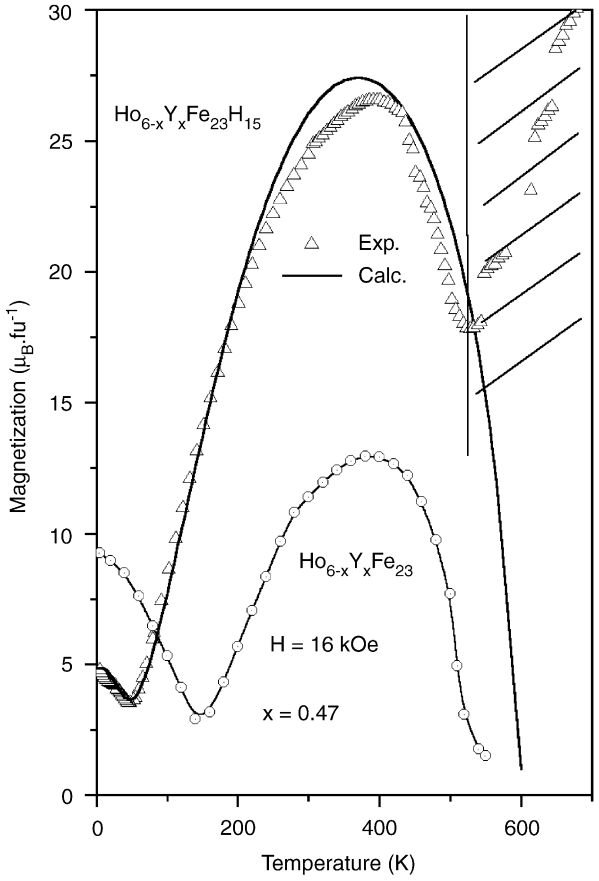

Fig. 3. Temperature variations of magnetization at 16 kOe of $Ho_{6-x}Y_xFe_{23}$ and $Ho_{6-x}Y_xFe_{23}H_{15}$ ($x = 0.47$) up to 700 K. Solid line are calculated values (see text). The hatched area corresponds to a temperature decomposition zone of the hydride.

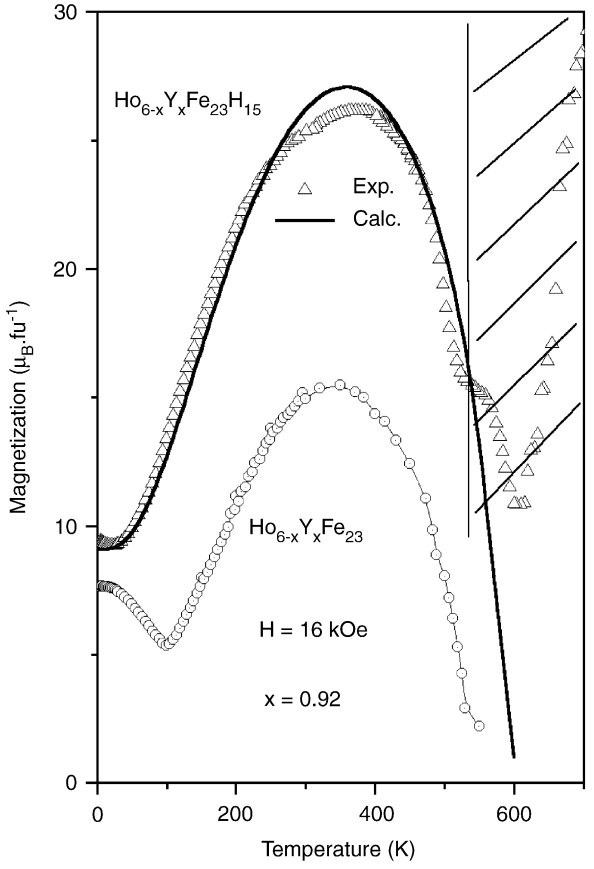

Fig. 4. Temperature variations of magnetization at 16 kOe of $Ho_{6-x}Y_xFe_{23}$ and $Ho_{6-x}Y_xFe_{23}H_{15}$ ($x = 0.92$) up to 700 K. Same legend as Fig. 3.

corresponding hydride is slightly beyond or at the limit to present a compensation temperature. Due in part to small differences between sublattices magnetizations, the compensation temperature is a zone of canted magnetic structures [11,12].

3.2. Magnetization results above 300 K

Above room temperature, the measured magnetic properties depend on chemical stability of the hydrides. Three temperature zones may be distinguished (Figs. 3 and 4): Below ~400 K, reversible measurements indicate that the hydrides are stable. In this temperature area, magnetization of both compounds present a maximum which is more than twice larger as that of corresponding alloys. Between 400 and ~550 K, the hydrides are desorbing hydrogen as indicated by irregularities in the $M(T)$ curves. Finally, decomposition of the hydrides occured above ~550 K (hatched areas in Figs. 3 and 4): X-ray diffraction experiments performed on the samples after 700 K measurements show the presence of metallic Fe. Nevertheless, extrapolation of magnetization curves (Figs. 3 and 4) indicate that Curie temperature of the hydrides—approximately $T_C \sim 600$ K for both compounds—is larger than that of parent alloys.

3.3. Magnetization temperature dependence

The preceding results (large increase of magnetizations above T_{comp}, decreasing of T_{comp}, increase of T_C) are mainly related to an increase of the iron magnetic moment μ_{Fe} upon hydrogenation of the parent alloy [2,6–8]. Recently, in the YFe_2H_z system, analyses of the density of states (DOS) provides new insight for the role played by hydrogen as to the increase of μ_{Fe} [13]. In comparison to its parent alloy, the increase of μ_{Fe} and the larger 4.2 K hydride magnetic moment corresponding to $x = 0.92$ (Fig. 4) allow thus to conclude that the compound presents no compensation point ($T_{comp} < 4.2$ K is very unlikely).

Moreover, the decreasing of the compensation temperature T_{comp} was also qualitatively ascribed to a weakening in the exchange coupling N_{R-Fe} between the R and Fe sublattices [14,15]. In order to obtain a more quantitative analysis, we propose to interpret the

magnetic properties of $Ho_{6-x}Y_xFe_{23}H_{15}$ compounds on the basis of Néel molecular field model for a two R and T sublattices ferrimagnet with the introduction of a canting angle θ as developped by Herbst and Croat [9]. Using this model, the resultant magnetization of the compound M_{tot} is given by

$$\vec{M}_{tot}(T) = \vec{M}_{Fe}(T) + \vec{M}_R(T), \quad (1)$$

where $\vec{M}_{Fe}$ and $\vec{M}_R$ are the sublattices magnetizations deviating from anticollinearity by a temperature-independent canting angle θ· The value of θ is comprised between 0 (anticollinearity) and θ_{max} corresponding to the largest canting angle allowing $\vec{M}_{tot}$, $\vec{M}_R$ and $\vec{M}_{Fe}$ to form a closed triangle, i.e,

$$\theta_{max} = \sin^{-1}(M_{tot}/M_R). \quad (2)$$

In a first approximation, this model may be extended to the pseudo binary system $Ho_{6-x}Y_xFe_{23}H_{15}$:

$$\vec{M}_{tot}(T,x) = \vec{M}_{Fe}(T,x) + \vec{M}_R(T,x). \quad (3)$$

The sublattice where the substitution takes place (here Ho and Y) being treated as one sublattice [12] of magnetization:

$$M_R(0,x) = (6-x)gJ, \quad (4)$$

where $g = 5/4$ and $J = 8$ for free Ho^{3+} ion, and θ corresponds to the mean canting angle of the Ho moments relative to M_{Fe} influenced by yttrium substitution.

The magnetic properties $M(H, T, x)$ are calculated according to the following equation:

$$M_i(T) = M_i(T=0)B_{Ji}(u_i), \quad i = \text{Ho, Fe}, \quad (5)$$

where $M_i(T) = n_i\mu_i(T)$ represents the magnetization of the n_i magnetic ions of moment μ_i at temperature T in units of the Bohr magneton (μ_B), B_{Ji} being the Brillouin function, $J_{Fe} = 1$ [9], $J_{Ho} = 8$ (Ho^{3+}), and

$$u_i = m_i(0)\cdot H_i(T)/kT, \quad (6a)$$

$$H_i(T) = H_a + (N\mu_B\rho/M_w)\sum_j n_i N_{ij}\mu_j(T), \quad (6b)$$

where H_a represents the applied field, N is Avogadro's number, ρ the density, and M_w is the molecular formula weight of the compound. N_{ij} are the molecular field coefficients ($N_{ij} = N_{ji}$).

In order to have a minimum of parameters, we assume that the 4.2 K iron magnetic moment is close to its mean value $\mu_{Fe} \approx 2.3\,\mu_B$ at.$^{-1}$ deduced from neutron diffraction data in $Ho_6Fe_{23}D_{15.7}$ compound [8]. The Curie temperature T_C allows the determination of N_{Fe-Fe} magnetic exchange parameter [5,9]. In case of hydrides, experimental T_C are not available. We put a lower limit on N_{Fe-Fe} by choosing the same values as those of parent alloys [5] (Table 1). θ, which is temperature independent in the model, may be obtained from 4.2 K hydrides magnetization values using Eq. (1).

Table 1
Experimental data and parameters used for calculation of the magnetization of $Ho_{6-x}Y_xFe_{23}H_{15}$

X	T_{comp} (K)	μ_{Fe} (μ_B at^{-1})	θ (°)	θ_{max} (°)	N_{Fe-Fe}	N_{Ho-Fe}	N_{Ho-Ho}
0[a]	75	2.3	3	7	5200	−500	100
0.47	50	2.27	4	6	5314	−550	100
0.92	—	2.27	10	11	5424	−650	50

[a] Experimental data of Ref. [6].

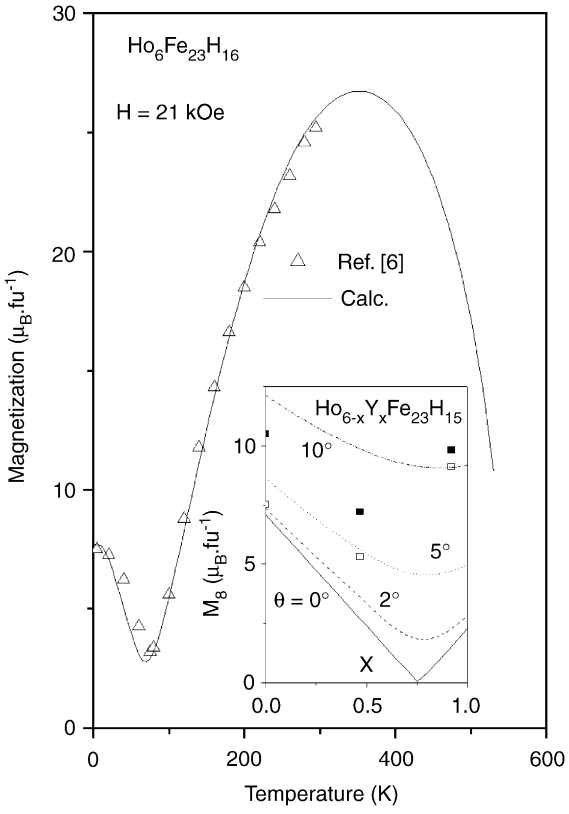

Fig. 5. Temperature variations of magnetization at 21 kOe of $Ho_6Fe_{23}H_{15}$ (Ref. [6]). Solid lines are calculated values. Inset: magnetization at 4.2 K and 16 kOe (empty squares) of the hydrides $Ho_{6-x}Y_xFe_{23}H_{15}$ versus calculated values for different values of canting angle θ. Solid squares are calculated magnetizations for the maximum canting angle θ_{max}.

We plotted in Fig. 5 the concentration dependence of calculated magnetization moments M_{tot} (4.2 K, 16 kOe) for different values of θ. We observe that the experimental magnetization data correspond to increasing values of θ when yttrium concentration x increases. Nevertheless, $\theta \leqslant 10°$, the maximum being obtained for $x = 0.92$ (10°). In Fig. 5, we plotted also the calculated magnetization moment $M_{tot}(\theta_{max})$ corresponding to θ_{max}, the maximum possible canting angle compatible with experiments (Eq. (2)). Experimental M_{tot} is close to $M_{tot}(\theta_{max})$ only when $x = 0.92$. This yttrium concentration is in the vicinity of $x \sim 0.75$ which is the hydride

composition for which $T_{comp} = 0$ K. This corresponds generally to large canting angles [5,9].

The different parameters are summarized in Table 1. The exchange parameters N_{Ho-Fe} and N_{Ho-Ho} are deduced from a least-squares fit of the experimental magnetization values of the hydrides using Eqs. (1)–(6). The calculated results are presented in Figs. 3–5 for $x =$ 0.47, 0.92 and 0, respectively. As can be observed, the agreement is rather good indicating that the different assumptions used in the model are reasonable. Particularly at T_{comp}, the calculated $M(T_{comp})$ moment is close to its experimental value, in agreement with the assumed temperature independency of θ. The present results confirm the assumed weakening of the exchange coupling N_{Ho-Fe} [14,15]. In effect (Table 1), for all hydrides, $|N_{Ho-Fe}|_{hydride} < |N_{Ho-Fe}|_{alloy}$ as $N_{Ho-Fe} = -750$ for parent intermetallic compounds

4. Conclusion

Magnetization measurements performed on ferrimagnetic $Ho_{6-x}Y_xFe_{23}H_{15}$ hydrides show the influence of hydrogenation on the magnetic properties of parent alloys: decreasing of the compensation temperature, large increase of the Curie temperature and of magnetization of the compounds above T_{comp}, in relation to an increase of the iron magnetic moment and weakening of Ho–Fe exchange interactions. Within the frame of Herbst and Croat refined-Néel ferrimagnetic model, the mean canting angle θ ($\theta \leqslant 10^\circ$) reflects the importance of canted magnetic structures between R and Fe sublattices. For unsubstituted $Ho_6Fe_{23}H_{15}$ ($x = 0$), this influence is weak, in contrast to yttrium-substituted hydrides, particularly for composition in the vicinity of $T_{comp} \sim 0$ K. It is to be noted that a large canting angle $\theta = 20.2^\circ$ was obtained for Tm_6Fe_{23} for which $T_{comp} = 0$ [9]. θ may reflect equally the crystallographic disorder introduced by yttrium substitution in the Ho sublattice.

References

[1] H. Le Gall, R. Sbiaa, S. Pogossian, J. Alloys Compds. 275–277 (1998) 677.
[2] E. Burzo, A. Chelkowski, H.R. Kirchmayr, H.P.J. Wijn (Eds.), Landolt-Börnstein Group III, Vol. 19–d2, Springer, Berlin, 1990.
[3] M.B. Harris, G.A Stewart, D.C. Creagh, Solid State Commun. 85 (1993) 389.
[4] G.A. Stewart, D.C. Creagh, J. Phys. F: Met. Phys. 15 (1985) 1639.
[5] J. Ostorero, J. Alloys Compds. 317–318 (2001) 450.
[6] E.B. Boltich, F. Pourarian, W.E. Wallace, H.K. Smith, S.K. Malik, Solid State Common. 40 (1981) 117.
[7] W.E. Wallace, F. Pourarian, A.T. Pedziwiatr, E.B. Boltich, J. Less Common Met. 130 (1987) 33 (Experiments performed on $Ho_6Fe_{23}D_z$).
[8] J.J. Rhyne, K. Hardman-Rhyne, H.K. Smith, W.E. Wallace, J. Less Common Met. 94 (1983) 95 (Experiments performed on $Ho_6Fe_{23}D_z$).
[9] J.F. Herbst, J.J. Croat, J. Appl. Phys. 55 (1984) 3023.
[10] V. Paul-Boncour, M. Latroche, L. Guénée, A. Percheron-Guégan, B. Ouladdiaf, F. Bourée-Vigneron, J. Solid State Chem. 142 (1999) 120.
[11] A. Sarkis, E. Callen, Phys. Rev. B 26 (1982) 3870 and references therein.
[12] G. Hilsher, H. Rais, J. Phys. F: Met. Phys. 8 (1978) 511.
[13] S.F. Matar, V. Paul-Boncour, C. R. Acad. Sci. Paris IIc 3 (2000) 27.
[14] F. Ishikawa, I. Yamamoto, M. Yamaguchi, M.I. Bartashevich, T. Goto, J. Alloys Compds. 253–254 (1997) 350.
[15] K. Matsuda, I. Yamaguchi, H.A. Yamamoto, T. Katori, M.I. Goto, Bartashevich, J. Alloys Compds. 231 (1995) 201.